CHALMERS
UNIVERSITY OF TECHNOLOGY

Energy Efficient Optimization-Based Coordination of Electric Automated Vehicles in Confined Areas

Citation for the original published paper (version of record):
Kojchev, S., Hult, R., Fredriksson, J. (2023). Energy Efficient Optimization-Based Coordination of Electric Automated Vehicles in Confined
Areas. Proceedings of the IEEE Conference on Decision and Control: 3433-3440.
http://dx.doi.org/10.1109/CDC49753.2023.10383878

Energy efficient optimization-based coordination of electric automated vehicles in confined areas

Stefan Kojchev[1], Robert Hult[2] and Jonas Fredriksson[3]

***Abstract*— In this paper, we present an optimization-based control strategy for coordinating multiple electric automated vehicles (AVs) in confined sites. The approach focuses on obtaining and keeping energy-efficient driving profiles for the AVs while avoiding collisions in cross-intersections, narrow roads, and merge crossings. Specifically, the approach is composed of two optimization-based components. The first component obtains the energy-efficient profiles for each individual AV by solving a Nonlinear Program (NLP) for the vehicle's complete mission route. The conflict resolution, which is performed by the second component, is accomplished by solving a time-scheduling Mixed Integer Linear Programming (MILP) problem that exploits the application characteristics. We demonstrate the performance of the algorithm through a non-trivial comparative simulation example with an alternative optimization-based heuristic.**

I. INTRODUCTION

Confined areas, such as ports, logistic centers, mines, etc., are deemed as use cases for the near-future deployment of automated vehicles (AVs) as they void some of the barriers that exist in deploying automated vehicles on public roads [1]. In particular, in confined areas, there are no external non-controlled actors, which drastically reduces safety concerns. One of the public road challenges that persist in confined areas is the safe and efficient coordination of AVs in MUTually EXclusive (MUTEX) zones. Adequate coordination can lead to improved energy efficiency and considerable increases in productivity. Enhancing energy efficiency is an important goal particularly due to the industry's demand for incorporating electric vehicles on sites.

For public roads, the coordination of automated vehicles for intersection MUTEX zones has received substantial attention, see [2] for a comprehensive survey. In general, the coordination problem is difficult to solve and is formally shown to be NP-hard in [3]. Each MUTEX zone implies that there should be an order in which the vehicles cross the zone. This combinatorial decision is the predominant component in the complexity of the coordination problem. Commonly proposed approaches leverage optimal control methods, often relying on simplifying assumptions and heuristics, to determine the crossing order and to compute the coordinated vehicle trajectories, see [4], [5], [6], [7].

This work is partially funded by Sweden's innovation agency Vinnova, project number: 2018-02708.

[1]Stefan Kojchev is with Volvo Autonomous Solutions and the Mechatronics Group, Systems and Control, Chalmers University of Technology stefan.kojchev@volvo.com; kojchev@chalmers.se

[2]Robert Hult is with Volvo Autonomous Solutions, 41873 Göteborg, Sweden robert.hult@volvo.com

[3]Jonas Fredriksson is with the Mechatronics Group, Systems and Control, Chalmers University of Technology, 41296 Göteborg, Sweden jonas.fredriksson@chalmers.se

Vehicles in confined areas, on the other hand, have additional MUTEX zones besides intersections, such as narrow roads, merge-splits, work-stations (e.g., loading/unloading zones, crushers, etc.), and charging stations. In confined sites, the vehicles are assigned transport missions such as transporting goods from point A to B within specified time limits. Fortunately, compared to the public road scenario the full site layout of the confined area is known, i.e., for each vehicle, the entire route is known. Consequently, it is possible to plan the motion of the vehicles from the start of a transport mission to its end. Planning the motion over long horizons is particularly beneficial in terms of energy efficiency, see e.g. [8]. Another distinguishing factor of the confined areas application case is that a single vehicle can experience multiple combinations of the MUTEX zones along its route, i.e., the vehicle can have multiple intersections, narrow roads, charging stations, etc. The authors [9] and [10] propose approaches on multiple intersection coordination, however, they consider a "cut-out" around the intersections with vehicles arriving at speed in comparison to the desired full route motion planning. For applications at confined site areas, a central computation unit and good communication coverage can be assumed. For this reason, and the above-stated application requirements, we believe that a centralized approach that computes a high-level motion plan for all vehicles is a favorable coordination strategy. The computed plan would then be tracked by a low-level controller on the individual vehicle.

The coordination problem for valet parking applications has a lot of similarities with the confined site coordination problem, as both applications consider closed-off areas where the vehicles can experience multiple MUTEX zones of different types, [11], [12]. The approach in this paper presents an alternative optimization-based heuristic. Furthermore, the valet parking applications have laxer energy efficiency and productivity goals, as well as the restriction that the vehicles move at lower speeds.

In our previous work, [13] and [14], we have proposed different heuristics that decompose the coordination problem in a Mixed Integer Quadratic Program (MIQP) that is tasked with obtaining an optimal crossing order for the MUTEX zones and a central continuous Nonlinear Program (NLP) that is solved for the optimal vehicle trajectories. The approach in this paper tackles the problem in a similar way, but with a particular focus on energy efficiency. In essence, we aim to "split" the problem with one part of the solution aiming at obtaining the energy-efficient trajectories and the other part dealing with the combinatorial problem connected

to the MUTEX occupancy or crossing order. The energy-efficient trajectories are computed by solving an NLP for all vehicles individually, where the motion profile is not constrained by the occupancy constraints. The goal of this approach is to minimize deviations in the energy-efficient profiles while avoiding all possible conflicts in the MUTEX zones.

A transport mission for vehicles in confined site areas is characterized by mission start and end time bounds, meaning that the vehicles could leave their start point in some time interval as long as they arrive at their end destination in the desired time-bound. Making use of the mission start time flexibility, it is favorable to form the MUTEX conflict resolution problem as a time-scheduling problem. Scheduling problems can be solved by converting them to a Mixed Integer Linear Programming (MILP) as for example done in [15] and [16]. The MILP in this paper is formed as finding a mission start time such that all occupancy conflicts are avoided while the energy-efficient profile is kept. The proposed heuristic differs from approaches in literature due to the confined area specifics, which in essence are the centralized long-horizon energy-efficient planning with conflict resolution for all existing MUTEX zones. In comparison to [13] and [14] the approach in this paper differs by solving a time-scheduling MILP instead of a MIQP and the approach in this paper will maintain the energy-efficient profiles of the vehicles by utilizing the mission start time flexibility. To mitigate infeasibilities when conflicts cannot be avoided by only delaying the mission start time, the approach is capable of modifying the energy-efficient trajectories by obtaining new MUTEX entry and exit times. The results of the approach are compared with the heuristic proposed in [14], in a non-trivial simulation example.

II. VEHICLE DYNAMICS

In this section, the longitudinal dynamics that describe the motion of the electric automated vehicles are derived. For the rest of this paper, we consider a road network of N_a fully automated vehicles traversing in a fully confined area, meaning that non-controlled traffic participants such as pedestrians, manually operated vehicles, bicycles, etc., are absent. Furthermore, we assume that the routes of the vehicles through the road network are known, that no vehicle reverses, and that overtakes are prohibited.

A. Longitudinal Dynamics

For an electric vehicle $i \in 1, ..., N_a$, the longitudinal dynamics can be described, using Newton's laws of motion, as

$$\dot{p}_i(t) = v_i(t), \tag{1a}$$

$$\dot{v}_i(t) = \frac{1}{m_i}\left(F_{M,i}(t) + F_{b,i}(t) - F_{d,i}(v_i,t) - F_{rg,i}(p_i,t)\right), \tag{1b}$$

where p_i, v_i and m_i are vehicle i's position, velocity and mass, respectively. The forces are the motor force $F_{M,i}$, the force generated by the friction brakes $F_{b,i}$, the aerodynamic drag $F_{d,i}$ and the rolling resistance and gravitational force $F_{rg,i}$. The aerodynamic drag and the rolling resistance and gravitational force can be described as

$$F_{d,i}(v_i,t) = \frac{1}{2}\rho A_i c_{a,i} v_i(t)^2 \tag{2a}$$

$$F_{rg,i}(p_i,t) = m_i g(sin(\theta(p_i(t))) + c_{r,i} cos(\theta(p_i(t)))), \tag{2b}$$

where ρ is the air density, A_i is the frontal area of the vehicle, $c_{a,i}$ is the aerodynamic drag coefficient, $c_{r,i}$ is the rolling resistance coefficient and θ is the road gradient.

As stated in [14], it is beneficial to state the dynamics in the spatial domain as it is favorable to optimize the trajectories of the vehicles over their full path. Using that $\frac{\mathrm{d}p_i}{\mathrm{d}t} = v_i(t)$ and $\mathrm{d}t = \mathrm{d}p_i / v_i(t)$, leads to the travel time t_i as a state whereas the position is now the independent variable. The vehicle dynamics (1) in the spatial domain thus are

$$\frac{\mathrm{d}t_i}{\mathrm{d}p_i} = \frac{1}{v_i(p_i)} \tag{3a}$$

$$\frac{\mathrm{d}v_i}{\mathrm{d}p_i} = \frac{1}{v_i(p_i)}\frac{1}{m_i}(F_{M,i}(p_i) + F_{b,i}(p_i) - \frac{1}{2}\rho A_i c_{a,i} v_i(p_i)^2 - m_i g(sin(\theta(p_i)) + c_{r,i} cos(\theta(p_i)))). \tag{3b}$$

Note that (3a) imposes that the velocity must be strictly positive.

B. Velocity and Acceleration Constraints

In addition to the minimum velocity constraint coming from the model, we upper bound the velocity in order to obey speed limits:

$$\underline{v}_i \leq v_i(p_i) \leq \overline{v}_i. \tag{4}$$

Furthermore, we bound the longitudinal acceleration of the vehicle, $a_i(p_i) = \frac{\mathrm{d}v_i}{\mathrm{d}p_i}$, that is obtained from (3b)

$$\underline{a}_{i,\text{lon}} \leq a_i(p_i) \leq \overline{a}_{i,\text{lon}}, \tag{5}$$

and impose constraints resulting from the curvature of the road. When the vehicles operate on curved roads they experience lateral forces. As the one-dimensional model that is used in this paper does not account for lateral motion, the following constraint is enforced

$$\left(\frac{a_i(p_i)}{\overline{a}_{i,\text{lon}}}\right)^2 + \left(\frac{\kappa_i(p_i) v_i(p_i)^2}{\overline{a}_{i,lat}}\right)^2 \leq 1, \tag{6}$$

where $\overline{a}_{i,lat}$ is the lateral acceleration limit and $\kappa_i(p_{i,k})$ is the road curvature, that is assumed to be available at every point along the path.

Additionally, the braking force $F_{b,i}(p_i)$ is constrained by its mechanical limits, i.e.,

$$\underline{F}_{b,i}(p_i) \leq F_{b,i}(p_i) \leq 0 \tag{7}$$

C. Electric Machine and Battery

The powertrain of an electric vehicle typically consists of a battery connected to an electric machine (EM) that drives the wheels. In general, the EM can operate both in traction mode, by drawing energy from the battery for propulsion, and as a generator, by restoring part of the kinetic energy back into the battery when the vehicle decelerates. The longitudinal force of vehicle $i \in 1, ..., N_a$ and its velocity can be related to the motor torque $T_{M,i}$ and the rotational speed $w_{M,i}$ through:

$$T_{M,i}(p_i) = \frac{r_{w,i}\eta(F_{M,i})}{M_{f,i}} F_{M,i}, \;\; \omega_{M,i}(p_i) = \frac{M_{f,i}}{r_{w,i}} v_i(p_i), \tag{8}$$

where $r_{w,i}$ is the wheel radius, $M_{f,i}$ is the transmission's gear ratio, and $\eta(F_{M,i})$ is the final gear efficiency function. It has a value of $1/\eta_f$ when the EM operates as a motor and η_f when the EM operates as a generator, where η_f is the efficiency coefficient of the final gear. Due to the power limitations of the motor, the torque has to satisfy the constraint:

$$|T_{M,i}(p_i)| \leq \min(T_{\text{max,i}}, P_{\text{max,i}}/\omega_{M,i}(p_i)), \tag{9}$$

where $T_{\text{max,i}}$ is the maximum motor torque and $P_{\text{max,i}}$ is the maximum power that the motor can supply.

An issue with this formulation is that the torque is not differentiable when switching between its traction and generator modes. A practical workaround is by splitting the EM force by adding separate force variables for each operating mode, i.e., $F_{M,i}(p_i) = F_{\text{trac},i}(p_i) - F_{\text{gen},i}(p_i)$, with $F_{\text{trac},i}(p_i)$ indicating the traction mode force and $F_{\text{gen},i}(p_i)$ the generator force. These forces are then bounded by

$$0 \leq F_{\text{trac},i}(p_i) \leq \frac{T_{\text{max,i}} M_{f,i} \eta_f}{r_{w,i}} \tag{10a}$$

$$0 \leq F_{\text{gen},i}(p_i) \leq \frac{T_{\text{max}} M_{f,i}}{\eta_f r_{w,i}}. \tag{10b}$$

The battery is modeled as an open circuit voltage connected in series to an internal resistance. The internal battery power can then be defined as a nonlinear function $P_{b,i}\left(\omega_{m,i}, T_{M,i}\right)$, as in e.g. [17]. With that, we can assemble our complete definition of the longitudinal vehicle dynamics as

$$\frac{\mathrm{d}t_i}{\mathrm{d}p_i} = \frac{1}{v_i(p_i)} \tag{11a}$$

$$\begin{aligned}\frac{\mathrm{d}v_i}{\mathrm{d}p_i} = \frac{1}{v_i(p_i)} \frac{1}{m_i} (&F_{\text{trac},i}(p_i) - F_{\text{gen},i}(p_i) + F_{b,i}(p_i) \\ &- \frac{1}{2}\rho A_i c_{a,i} v_i(p_i)^2 - m_i g(sin(\theta(p_i)) + c_{r,i} cos(\theta(p_i)))),\end{aligned} \tag{11b}$$

resulting in the state vector $x_i(p_i) = [t_i(p_i), v_i(p_i)]$ and the input vector $u_i(p_i) = [F_{\text{trac},i}(p_i), F_{\text{gen},i}(p_i), F_{b,i}(p_i)]$.

III. OPTIMAL CONTROL PROBLEM

In this section, we define the safety constraints for the MUTEX zones and form the energy-efficient vehicle coordination problem using the model developed in the previous section. The road network is consistent with MUTEX zones such as cross-intersections, narrow roads, and merge crossings. Motivated by the properties of the confined area, such as a centralized computing unit and communication, the problem is stated as an optimal control problem (OCP) that computes the collision-free vehicle trajectories.

A. Safety Constraints

The safety constraints ensure a collision-free crossing of the MUTEX zones, that the vehicles encounter. In this paper, we consider three types of conflict zones, the "intersection-like", narrow road and merge-split depicted in Figure 1. A MUTEX zone is defined by the entry and exit position $[p_i^{in}, p_i^{out}]$ on the path of each vehicle. From the known positions, the time of entry and exit of vehicle i is $t_i^{in} = t_i(p_i^{in})$ and $t_i^{out} = t_i(p_i^{out})$, respectively.

1) Narrow road and intersection-like zones: In the narrow road MUTEX zones, Figure 1-b), two or more vehicles are arriving at the zone from opposite directions of travel. From a safety perspective, this translates to "reserving" the zone for one or more vehicles coming from the same direction. The vehicles coming from the opposite direction are not allowed to occupy the zone until it is vacated. The intersection-like MUTEX zone, Figure 1-a), is similar to the narrow road in terms of its safety requirement, i.e., vehicle j is not allowed to enter the MUTEX zone before vehicle $i \neq j$ exits the MUTEX zone, or vice-versa.

We let $\mathcal{I} = \{I_1, I_2, ..., I_{r_0}\}$ denote the set of all intersections and narrow roads in the confined area, with r_0 being the total number of intersection and narrow road CZs, and $\mathcal{Q}_r = \{q_{r,1}, q_{r,2}, ..., q_{r,l}\}$ denote the set of vehicles that cross an intersection or narrow road I_r. The order in which the vehicles cross the intersection I_r is denoted $\mathcal{O}_r^{\mathcal{I}} = \left(s_{r,1}, s_{r,2}, ..., s_{r,|\mathcal{Q}_r|}\right)$, where $s_{r,1}, s_{r,2}, ...$ are vehicle indices and we let $\mathcal{O}^{\mathcal{I}} = \left\{\mathcal{O}_1^{\mathcal{I}}, \ldots, \mathcal{O}_r^{\mathcal{I}}\right\}$. A sufficient condition for collision avoidance for the r-th intersection or narrow road CZ can be formulated as

$$t_{s_{r,i}}(p^{\text{out}}_{s_{r,i}}) \leq t_{s_{r,i+1}}(p^{\text{in}}_{s_{r,i+1}}),\; i \in \mathbb{I}_{[1,|\mathcal{Q}_r|-1]}, \tag{12}$$

where t is determined from (11a).

2) Merge-split zones: In the merge-split case, Figure 1-c), two vehicles coming from different roads, but in the same direction of travel, join together on a common patch of road. After some distance, the roads separate. For these MUTEX zones, let $\mathcal{M} = \{M_1, M_2, ..., M_{w_0}\}$ denote a set of all merge-split zones, with w_0 being the total number of merge-split CZs in the site and $\mathcal{Z}_w = \{z_{w,1}, z_{w,2}, ..., z_{w,h}\}$ denote the set of vehicles that cross the merge-split CZ M_w. For efficiency, it is desirable to have several vehicles in the zone at the same time, instead of blocking the whole zone. This requires imposing rear-end collision constraints once the vehicles have entered the merge-split CZ. In this case, the order in which the vehicles enter the zone is denoted as $\mathcal{O}_w^{\mathcal{M}} = \left(s_{w,1}, s_{w,2}, ..., s_{w,|\mathcal{Z}_w|}\right)$, and we let $\mathcal{O}^{\mathcal{M}} = \left\{\mathcal{O}_1^{\mathcal{M}}, \ldots, \mathcal{O}_w^{\mathcal{M}}\right\}$. The collision avoidance requirement for the w-th merge-split CZ is described with the following

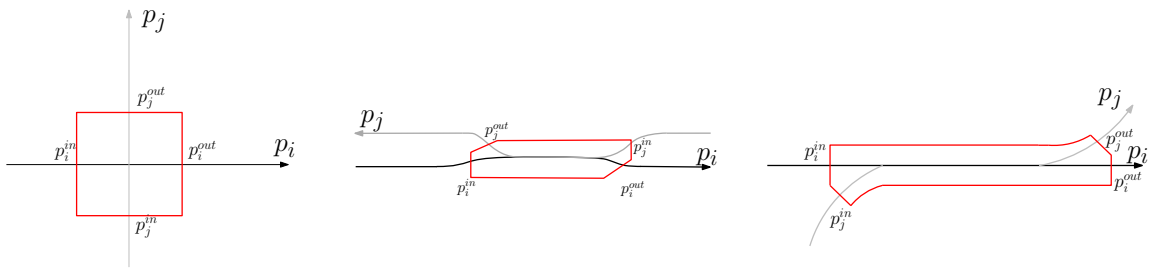

a) Intersection-like b) Narrow road c) Merge-split

Fig. 1. Types of conflict zones.

constraints:

$$t_{s_{w,i}}(p^{\text{in}}_{s_{w,i}}) + \Delta t \leq t_{s_{w,i+1}}(p^{\text{in}}_{s_{w,i+1}} - c) \tag{13a}$$

$$t_{s_{w,i},k_i} + \Delta t \leq t_{s_{w,i+1}}(p_{s_{w,i},k_i} - p^{\text{in}}_{s_{w,i}} + p^{\text{in}}_{s_{w,i+1}} - c),$$

$$k^{\text{in}}_{s_{w,i}} \leq k_i \leq k^{\text{out}}_{s_{w,i}} \tag{13b}$$

$$t_{s_{w,i}}(p^{\text{out}}_{s_{w,i}}) + \Delta t \leq t_{s_{w,i+1}}(p^{\text{out}}_{s_{w,i+1}} - c), \tag{13c}$$

$$i \in \mathbb{I}_{[1,|\mathcal{Z}_w|-1]},$$

where k_i is an index of the position vector $p_{s_{w,i}}$. The interpretation of eq. (13) is that while in the CZ, the vehicles must be separated by at least a time-period Δt and a distance c, depending on if vehicle j is in front of vehicle i or vice versa. This is equivalent to the standard offset and time-headway formulation often used in automotive adaptive cruise controllers.

B. Optimal Coordination Problem

With the defined vehicle model and safety constraints, we can now assemble the energy-efficient coordination of electric vehicles as an optimization problem. In essence, the problem of finding energy-efficient vehicle trajectories that avoid collisions can be stated as:

***Problem** 1:* (Energy-efficient coordination problem) Obtain the optimal state and control trajectories $\mathcal{X}^* = \{x_1^*, ..., x_{N_a}^*\}$, $\mathcal{U}^* = \{u_1^*, ..., u_{N_a}^*\}$, given the initial state $\mathcal{X}_0 = \{x_{1,0}, ..., x_{N_a,0}\}$, by solving the optimization problem

$$\min_{x_i, u_i, \mathcal{O}^{\mathcal{I}}, \mathcal{O}^{\mathcal{M}}} \sum_{i=1}^{N_a} \int_{p_{i,0}}^{p_{i,M_i}} \left(H_i a_i(p_i)^2 + Q_i P_{b,i}\right) \frac{1}{v_i(p_i)} \mathrm{d}p_i + R_i t_i(p_{i,M_i}) \tag{14}$$

$$\text{s.t} \quad \text{initial states} \;\; x_{i,0} = \hat{x}_{i,0}, \forall i$$
$$\text{system dynamics (11)}, \;\; \forall i$$
$$\text{state and input constraints (4)} - \text{(7)}, \text{(10)}, \;\; \forall i$$
$$\text{safety constraints (12)}, \;\; \text{(13)}, \forall i$$

where p_{i,M_i} indicates the end position for vehicle i, H_i, Q_i and R_i are the cost function weight parameters. For each vehicle, the cost function consists of minimizing the squares of the acceleration, the power of the battery, and the end time. The first two terms are related to energy-efficient driving while the last term motivates the vehicles to arrive at their end destination as fast as possible, i.e. productivity.

C. Discretization

The independent variable p_i is discretized as $p_i = (p_{i,0}, \ldots, p_{i,M_i})$, where the input is approximated using zero-order hold such that $u(p) = u_{i,k}, \; p \in [p_{i,k}, p_{i,k+1}[$. The equations are (numerically) integrated on the grid using an Explicit Runge-Kutta-4 (ERK4) integrator.

IV. TIME-SCHEDULING HEURISTIC

Problem 1 can be stated as a Mixed Integer Nonlinear Problem (MINLP), for which finding a solution is known to be difficult, especially for non-convex objectives or constraints [18]. A common procedure, as done in [7], is to split the problem by first solving for the combinatorial part, i.e., finding a crossing order for the MUTEX zones, and then after, solving a continuous NLP for the optimal trajectories with the found crossing order. For obtaining the crossing order, the heuristics in our previous work [13], [14] propose different approximations of the MINLP problem.

In this paper, we propose a solution heuristic with a focus on energy efficiency that exploits the application requirements. Specifically, we first solve (14) without the safety constraints for each vehicle individually instead of one centralized problem. By dropping the MUTEX zone constraints that couple the vehicles, the solution to each individual problem is not influenced by the behavior of the other vehicles. Thus, the obtained trajectories are the individual energy optimal trajectories for each vehicle. The goal of this heuristic is to keep the energy optimal trajectories while also satisfying the safety constraints. The next subsections give further information on how this is achieved.

A. Safety Constraints Reformulation

In confined areas the vehicles are given missions, for example, transfer X amount of load between points A and B, upon which their routes are decided. Furthermore, each mission is also specified by a mission start and end time-bound. In essence, $\underline{t}_i(p_{i,0}) \leq t_i(p_{i,0}) \leq \bar{t}_i(p_{i,0})$ and $\underline{t}_i(p_{i,M_i}) \leq t_i(p_{i,M_i}) \leq \bar{t}_i(p_{i,M_i})$. For simplicity, we are dropping the $(p_{i,0})$ notation meaning that $t_i(p_{i,0})$ is substituted by $t_{i,0}$. The safety constraints (12) can be reformulated w.r.t. $t_{i,0}$ as

$$t_{s_{r,i},0} + c^{\text{out}}_{s_{r,i}} \leq t_{s_{r,i+1},0} + c^{\text{in}}_{s_{r,i+1}}, \;\; i \in \mathbb{I}_{[1,|\mathcal{Q}_r|-1]}. \tag{15}$$

where $c^{\text{out}}_{s_{r,i}}$ and $c^{\text{in}}_{s_{r,i+1}}$ are the time constants that indicate the exit time for vehicle $s_{r,i}$ and entry for vehicle $s_{r,i+1}$, respectively. The time constants are obtained from the individual vehicle optimization problems.

Using the flexibility around the start time, for each vehicle, we can pose the collision avoidance problem by finding the start time $t_{i,0}$ such that the safety constraints are satisfied. If the start time is not upper-bounded, then there always exists a start time such that all collisions are avoided. For example, if two vehicles have a MUTEX zone, the collision can simply be avoided if one of the vehicles delays its departure until the other vehicle has exited the MUTEX zone. This indirectly will decouple the vehicles. However, in practice, the vehicles have an upper bound on their departure time. This means that in theory, it is possible even with the maximum delay of departure that a collision could happen between the vehicles when they keep their energy-efficient trajectories unchanged. One practical work-around can be to add additional variables to the safety constraints that provide extra time. In essence,

$$t_{s_{r,i}}(p_{s_{r,i},0}) + c^{\text{out}}_{s_{r,i}} \leq t_{s_{r,i+1}}(p_{s_{r,i+1},0}) + c^{\text{in}}_{s_{r,i+1}} + t^{\text{extra}}_{s_{r,i+1}}, \quad i \in \mathbb{I}_{[1,|\mathcal{Q}_r|-1]}. \tag{16}$$

The constraints (13) can be reformulated in a similar way:

$$\begin{aligned} &t_{s_{w,i},0} + c^{\text{in}}_{s_{w,i}} + \Delta t \leq t_{s_{w,i+1},0} + c^{\text{in}}_{s_{w,i+1}} + t^{\text{in,extra}}_{s_{w,i+1}} \\ &t_{s_{w,i},0} + c^{k_i}_{s_{w,i}} + \Delta t \leq t_{s_{w,i+1},0} + c^{k_i}_{s_{w,i+1}} + t^{k_i,\text{extra}}_{s_{w,i+1}}, \\ &\qquad\qquad k^{\text{in}}_{s_{w,i}} \leq k_i \leq k^{\text{out}}_{s_{w,i}} \\ &t_{s_{w,i},0} + c^{\text{out}}_{s_{w,i}} + \Delta t \leq t_{s_{w,i+1},0} + c^{\text{out}}_{s_{w,i+1}} + t^{\text{out,extra}}_{s_{w,i+1}}, \\ &\qquad\qquad i \in \mathbb{I}_{[1,|\mathcal{Z}_w|-1]}. \end{aligned} \tag{17}$$

B. Mixed Integer Linear Program

The MUTEX occupancy problem can be stated as a time-scheduling Mixed Integer Linear Program (MILP) in $\mathbf{T_0}$, $\mathbf{T}^{\text{extra}}$, where $\mathbf{T_0} = (t_{1,0}, \ldots, t_{N_a,0})$ and $\mathbf{T}^{\text{extra}} = (t^{\text{extra}}_1, \ldots, t^{\text{extra}}_{(2(r_0+w_0))})$:

$$\min_{\mathbf{T_0}, \mathbf{T}^{\text{extra}}} \quad \alpha \sum_{i=1}^{N_a} t_{i,0} + \beta \sum_{j=1}^{2(r_0+w_0)} t_j^{extra} \tag{18a}$$

$$\text{s.t} \quad (16),\ (17) \tag{18b}$$

$$\underline{t}_{i,0} \leq t_{i,0} \leq \overline{t}_{i,0} \tag{18c}$$

$$0 \leq t^{\text{extra}}_j \leq \overline{t}^{\text{extra}}_j, \tag{18d}$$

where α and β are the cost function weights, with $\beta \gg \alpha$. The integer constraints connected to (16) and (17) can be practically included, for example, by using the big-M technique [18]. The solution to this problem is the start times for all vehicles and, if necessary, extra time added to the MUTEX entry and exit times. The extra times are upper bounded by the maximum possible entry or exit time of the vehicle for that zone. The upper bound time is found if the vehicles move with $\underline{v}_i$ until the MUTEX zone. Non-zero extra time indicates that a collision for a vehicle cannot be avoided by only delaying the start time if that vehicle maintains its energy-efficient trajectory.

C. Recomputing Vehicle Trajectories

In the case of a non-zero extra time, we need to recompute the trajectory for the vehicle whose MUTEX times are influenced by the extra time. In essence, the vehicle needs to adjust its energy-efficient trajectory such that its new entry and exit times to the MUTEX zone are

$$t_n(p^{\text{in}}_{n,g}) = t_{n,0} + c^{\text{in}}_g + t^{\text{extra}}_g \tag{19a}$$

$$t_n(p^{\text{out}}_{n,g}) = t_{n,0} + c^{\text{out}}_g + t^{\text{extra}}_g, \tag{19b}$$

where the index n denotes the vehicle for which the recomputation is necessary, g is the MUTEX zone that has a non-zero extra time, and $c^{\text{in}}_g, c^{\text{out}}_g$ are the entry and exit time constants of the energy-efficient trajectories. Every vehicle with a non-zero extra time thus needs to solve an NLP problem including these constraints. In essence, the recomputation problem for vehicle n is

$$\begin{aligned} \min_{x_n, u_n} \quad & \int_{p_{n,0}}^{p_{n,M_n}} \left(H_n a_n(p_n)^2 + Q_n P_{b,n}\right) \frac{1}{v_n(p_n)} \mathrm{d}p_n \\ & + R_n t_n(p_{n,M_n}) \\ \text{s.t} \quad & \text{initial states } \ x_{n,0} = \hat{x}_{n,0} \\ & \text{system dynamics (11)}, \\ & \text{state and input constraints (4)} - \text{(7)}, \text{(10)}, \\ & \text{MUTEX entry and exit constraints (19)}, \end{aligned} \tag{20}$$

where the initial time is obtained from the solution of (18). The energy-efficient time-scheduling heuristic is summarized in Algorithm 1.

Algorithm 1 Energy-efficient time-scheduling heuristic

Input: $N_a, \mathcal{I}, \mathcal{Q}_r, \mathcal{M}, \mathcal{Z}_w$, vehicle paths

Output: $\mathcal{X}^*$, $\mathcal{U}^*$

1: $\forall i$: Obtain the energy optimal trajectories by solving NLP (14) w/o safety constraints (12),(13).
2: For all MUTEX zones extract the in and out time constants $c^{\text{in}}, c^{\text{out}}$ from the solution found in step 1.
3: Find $t_{i,0},\ i \in 1, \ldots N_a$ and $t^{\text{extra}}_j,\ j \in 1, \ldots 2(r_0 + w_0)$ by solving the MILP (18).
4: Recompute the vehicle trajectories
if $t^{\text{extra}}_j \neq 0$
1. Find the vehicle(s) and MUTEX zone(s) that need to be adjusted.
2. For the found vehicle(s) recompute the energy-efficient trajectories by solving NLP (20).
end if

V. NUMERICAL RESULTS

In this section, we present a simulation example using the heuristic described in Algorithm 1 and compare its performance to an alternative heuristic. In our previous work, [14] we proposed an approach that is based on a quadratic approximation of Problem 1 for obtaining the crossing order. The approximation is performed similarly to how Quadratic Programming (QP) sub-problems are formed in Sequential

TABLE I

INITIAL START TIMES FOR THE VEHICLES IN SECONDS.

$t_{1,0}$	$t_{2,0}$	$t_{3,0}$	$t_{4,0}$	$t_{5,0}$	$t_{6,0}$	$t_{7,0}$	$t_{8,0}$	$t_{9,0}$	$t_{10,0}$
1.5	0	1.1	0	54.3	49.1	0	117.5	0	5

Quadratic Programming (SQP), [19]. The result of the approximation is a Mixed Integer Quadratic Program (MIQP). The state and input trajectories are then calculated using the approximately optimal crossing order. The approach in [14] is summarized through Algorithm 2.

Algorithm 2 Two-stage approximation algorithm

Input: $N_a, \mathcal{I}, \mathcal{Q}_r, \mathcal{M}, \mathcal{Z}_w$, vehicle paths

Output: $\mathcal{X}^*$, $\mathcal{U}^*$

1: $\forall i$: Obtain a solution guess w_i^{**} by, solving NLP (14) w/o safety constraints (12),(13).

2: Using w_i^{**}, calculate and form the approximation terms that are necessary for the MIQP problem.

3: Solve the MIQP to get approximately optimal crossing orders $\hat{\mathcal{O}}^{\mathcal{I}}$, $\hat{\mathcal{O}}^{\mathcal{M}}$.

4: Solve a fixed-order NLP using $\hat{\mathcal{O}}^{\mathcal{I}}$, $\hat{\mathcal{O}}^{\mathcal{M}}$ to obtain $\mathcal{X}^*$, $\mathcal{U}^*$.

A. Simulation Setup

We consider the same confined site scenario as in [14] with the layout shown in Figure 2. In total there are ten vehicles on the site with two merge-split, two narrow roads, and sixteen intersection MUTEX zones. For both approaches the vehicle model, constraints, and optimization objectives are equivalent. Every vehicle starts from an initial velocity of 10 m/s and some vehicles start from a nonzero initial time to ensure that a collision occurs if no coordinating action is taken. The initial start times for all vehicles are summarized in Table I and these are the start time lower bounds ($\underline{t}_{i,0}$). The start time upper bound for all vehicles is $\bar{t}_{i,0} = 1800$ seconds, i.e., all the vehicles must start their mission in the next half an hour. The numerical values for the rest of the simulation parameters are summarized in Table II and are equivalent for all vehicles. The intersection CZ is created with a 5-meter margin ahead of and behind the collision point, whereas in the merge-split and narrow road CZ the margin is 15 meters for both the entry and exit points. For the merge-split CZ, it is desirable to keep at least a 0.5s margin between the vehicles, i.e. $\Delta t = 0.5$ in (13). We utilize the CasADi toolkit, [20], and IPOPT, [21], to formulate and solve the NLP optimization problems and use Gurobi for the MILP (18) and the MIQP problem in the comparative heuristic.

B. Discussion of Results

In the following, we compare the results of the two heuristics for this scenario. In particular, we compare the overall speed trajectories and reflect this comparison in terms of satisfying the safety constraints for one merge-split zone and one narrow road, as well as their influence on the overall objective cost. The presented MUTEX zones are encircled over in Figure 2.

TABLE II

SIMULATION PARAMETERS IN SI UNITS.

Parameter	N_a	m	ρ	A	c_a	c_r
Value	10	40000	1.18	8.36	1	0.0047
Parameter	$\underline{v}$	$\overline{v}$	$\underline{a}_{\text{lon}}$	$\overline{a}_{\text{lon}}$	$\overline{a}_{\text{lat}}$	$T_{\max}$
Value	0.1	25	-2	2	2	5614
Parameter	M_f	η_f	r_w	$\underline{F}_b$	$E_{b,\max}$	H
Value	2.8	0.98	0.49	-60000	395	1
Parameter	Q	R	α	β		
Value	20	5	1	100		

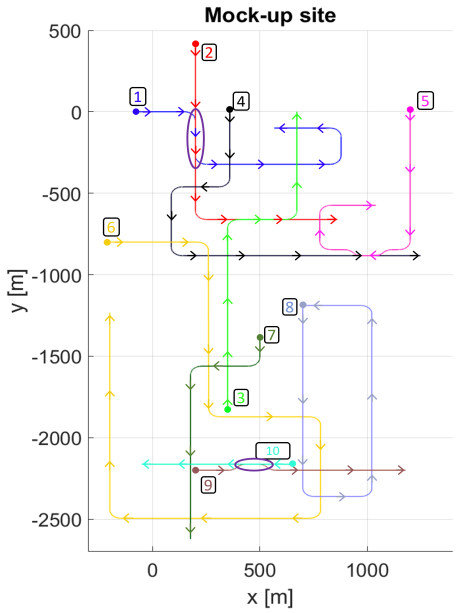

Fig. 2. Mock-up confined site area. The MUTEX zones that are investigated in the simulation scenario are encircled over in this figure.

Figure 3 depicts the speed profiles of the vehicles. The solid lines depict the results of the time-scheduling heuristic that aims to maintain the energy-efficient trajectories, while the dashed lines indicate the solution resulting from the MIQP-based approach as described in Algorithm 2. The MIQP-based approach is aware of all MUTEX zones the vehicles encounter and it is able to satisfy the safety constraints with minor speed changes well before the vehicle arrives at the MUTEX zone. In terms of performance, this behavior is beneficial, however, falls behind the time-scheduling heuristic that is able to satisfy the safety constraints and fully keep the energy-efficient speed profiles due to the start time flexibility.

Figure 4 shows the position vs. time trajectories of the two vehicles at the merge-split CZ. The trajectories are shifted such that a position of zero is the entry position in the MUTEX zone for both vehicles. The time is also shifted by the entry time of the first vehicle in the MUTEX zone (as it is the first vehicle to enter the zone). From the figure, we can observe that both approaches satisfy the safety constraint (13) as the vehicles are allowed to both occupy the zone at the same time and keep the desired gap between them. An interesting observation is that the time-scheduling approach delays the mission start time of the second vehicle such that

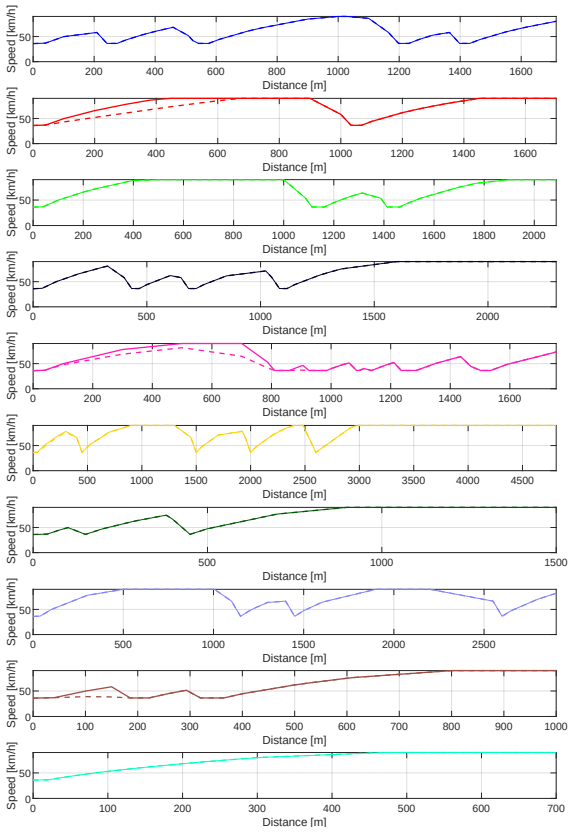

Fig. 3. Speed profiles resulting from the time-scheduling approach (solid lines) and resulting from the MIQP-based approach (dashed lines). In order to satisfy the safety constraints the MIQP-based approach has to deviate from the energy-efficient speed trajectories that are maintained by the time scheduling approach.

TABLE III

START TIMES FOR THE VEHICLES THAT SATISFY ALL SAFETY CONSTRAINTS FOUND WITH THE TIME-SCHEDULING APPROACH IN SECONDS.

$t_{1,0}$	$t_{2,0}$	$t_{3,0}$	$t_{4,0}$	$t_{5,0}$	$t_{6,0}$	$t_{7,0}$	$t_{8,0}$	$t_{9,0}$	$t_{10,0}$
1.5	5.71	1.1	0.14	60.9	49.1	0	118	2.8	5

the minimum gap is only kept at the exit point. This behavior enables the later entering vehicle to keep its energy-efficient speed profile.

It is worth highlighting that several collisions occur if the vehicles are not coordinated by either approach. When the vehicles are coordinated, either by the time-scheduling approach or the MIQP-based approach, all collisions are avoided. For sake of brevity, we refrain from depicting these results and refer the reader to [14] where the critical behavior is discussed in detail. For the time-scheduling approach, the initial mission start times for each vehicle that satisfy all safety constraints are summarized in Table III.

In terms of performance metric, the value of the objective function for the MIQP-based approach is 6764.84, while for the time-scheduling approach is 6532.01. Furthermore, in terms of energy efficiency, the time-scheduling approach leads to a 4 percent improvement in comparison to the MIQP-based approach. This might not seem like a drastic

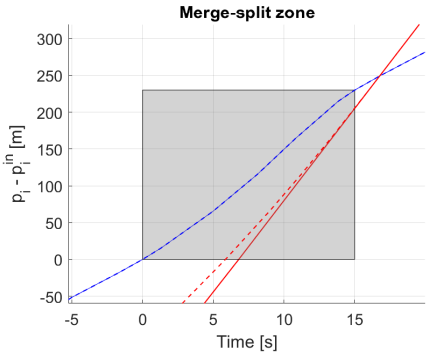

Fig. 4. Comparison of the crossings for the merge-split zone for the 1st and 2nd vehicle. The dashed lines are the MIQP-based trajectories and the full lines are the trajectories resulting from the time-scheduling algorithm.

difference, however, the vehicles typically have missions over long periods of time where even a slight one-mission improvement means, in general, significant long-term performance gain. Furthermore, the approaches have different computational complexities. The simulation scenario is implemented in MATLAB on a 2.90GHz Intel Xeon computer with 32GB of RAM. The first step for both approaches is the same, i.e., for all vehicles solving (14) without the safety constraints. This operation for the described scenario requires 1.02 seconds. For the MIQP-based approach, the MIQP problem requires 0.22 seconds and the fixed-order NLP 1.51 seconds. Meaning in total, the solve computational time for the approach described in Algorithm 2 is 2.75 seconds. For the time-scheduling approach, the MILP (18) is solved in 0.07 seconds and for this scenario setup, there is no need for recomputing any of the vehicles' trajectories as all extra times are equal to zero. The total computation time for this heuristic is thus 1.09 seconds and is a notable improvement. For confined area applications, due to the mission flexibility, we believe that in general there will be seldom a need to recompute the trajectories.

Remark 1: Recomputing vehicle trajectories. It is possible that the mission and scenario require extra time to be added to the MUTEX zone entry and exit times in order to not violate the safety constraints. In that case, the speed profiles for some (or all) vehicles need to be recomputed as explained in subsection IV-C. In the worst case, it is necessary to recompute N_a NLPs. The computational demand depends on the vehicle's path length as it is correlated to the horizon length. Figure 5 depicts the energy-efficient speed profile, the recomputed speed profiles as well as the MIQP-based speed profile for the narrow road between vehicles 9 and 10. This is an example when recomputation is necessary as the flexibility on the start time upper bound for vehicle 9 is tightened, thus resulting in the approach having to add extra time for vehicle 9 for the narrow road MUTEX zone. The recomputation time, i.e, the computation time for solving (20), is 0.149 seconds in the case when $\bar{t}_{9,0} = 2$ and 0.166 seconds when $\bar{t}_{9,0} = 0$. Figure 6 illustrates the safety constraint satisfaction for all speed profiles for this zone. The figure depicts the position-vs-position trajectory

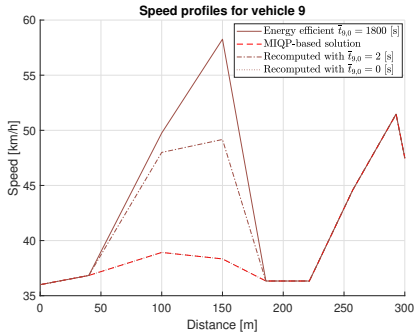

Fig. 5. Speed profile comparison for vehicle 9. The figure depicts the energy-efficient speed along with the recomputed speed profiles for tighter start time upper bounds and their deviation from the energy-efficient profile.

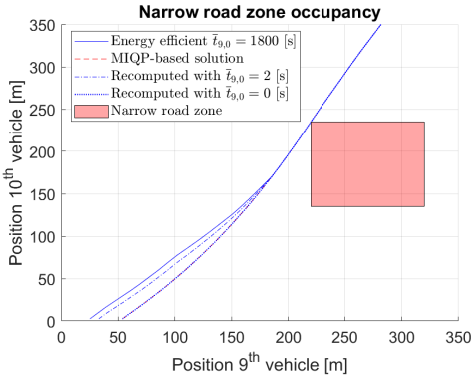

Fig. 6. The crossing of the narrow road MUTEX zone for different start time upper bounds. It is noticeable that all trajectories avoid violating the safety constraints for this zone, i.e., the depicted trajectories do not intersect the zone.

of the involved vehicles. The narrow road zone allows only one vehicle to occupy the zone at a time. For the trajectory dependency shown in the figure, this constraint entails that the trajectories must not intersect the zone. As can be seen, the approaches successfully manage to achieve the desired behavior. It can be noticed that when there is no flexibility in the start time the speed profile for the recomputed vehicle (vehicle 9) is equivalent to the speed profile resulting from the MIQP-based approach.

VI. CONCLUSIONS

In this paper, we have proposed an optimization-based approach that aims at computing energy-efficient solutions for the confined area coordination problem of electric automated vehicles. The approach optimizes the trajectories of the vehicles over their entire path while taking all collision zones into account. The comparative example demonstrates the performance benefits of the proposed approach, both in terms of improved energy efficiency and reduced computational effort. Future work will include charging and loading/unloading stations as part of the MUTEX zones as well as investigating the closed-loop behavior.

REFERENCES

[1] S. A. Bagloee, M. Tavana, M. Asadi, and T. Oliver, "Autonomous vehicles: challenges, opportunities, and future implications for transportation policies," *Journal of modern transportation*, vol. 24, no. 4, pp. 284–303, 2016.

[2] J. Rios-Torres and A. A. Malikopoulos, "A survey on the coordination of connected and automated vehicles at intersections and merging at highway on-ramps," *IEEE Transactions on Intelligent Transportation Systems*, vol. 18, no. 5, pp. 1066–1077, 2016.

[3] A. Colombo and D. Del Vecchio, "Efficient algorithms for collision avoidance at intersections," in *Proceedings of the 15th ACM international conference on Hybrid Systems: Computation and Control*, 2012, pp. 145–154.

[4] G. R. Campos, P. Falcone, H. Wymeersch, R. Hult, and J. Sjöberg, "Cooperative receding horizon conflict resolution at traffic intersections," in *53rd IEEE Conference on Decision and Control*. IEEE, 2014, pp. 2932–2937.

[5] A. Katriniok, P. Kleibaum, and M. Joševski, "Distributed model predictive control for intersection automation using a parallelized optimization approach," *IFAC-PapersOnLine*, vol. 50, no. 1, pp. 5940–5946, 2017.

[6] Y. J. Zhang, A. A. Malikopoulos, and C. G. Cassandras, "Optimal control and coordination of connected and automated vehicles at urban traffic intersections," in *2016 American Control Conference (ACC)*. IEEE, 2016, pp. 6227–6232.

[7] R. Hult, M. Zanon, S. Gras, and P. Falcone, "An miqp-based heuristic for optimal coordination of vehicles at intersections," in *2018 IEEE Conference on Decision and Control (CDC)*. IEEE, 2018, pp. 2783–2790.

[8] A. Hamednia, N. K. Sharma, N. Murgovski, and J. Fredriksson, "Computationally efficient algorithm for eco-driving over long look-ahead horizons," *IEEE Transactions on Intelligent Transportation Systems*, 2021.

[9] M. Hausknecht, T.-C. Au, and P. Stone, "Autonomous intersection management: Multi-intersection optimization," in *2011 IEEE/RSJ International Conference on Intelligent Robots and Systems*. IEEE, 2011, pp. 4581–4586.

[10] B. Chalaki and A. A. Malikopoulos, "Time-optimal coordination for connected and automated vehicles at adjacent intersections," *IEEE Transactions on Intelligent Transportation Systems*, 2021.

[11] H. Banzhaf, D. Nienhüser, S. Knoop, and J. M. Zöllner, "The future of parking: A survey on automated valet parking with an outlook on high density parking," in *2017 IEEE Intelligent Vehicles Symposium (IV)*. IEEE, 2017, pp. 1827–1834.

[12] M. Kneissl, A. K. Madhusudhanan, A. Molin, H. Esen, and S. Hirche, "A multi-vehicle control framework with application to automated valet parking," *IEEE Transactions on Intelligent Transportation Systems*, vol. 22, no. 9, pp. 5697–5707, 2020.

[13] S. Kojchev, R. Hult, and J. Fredriksson, "Optimization based coordination of autonomous vehicles in confined areas," in *2022 IEEE 25th International Conference on Intelligent Transportation Systems (ITSC)*. IEEE, 2022, pp. 1957–1963.

[14] S. Kojchev, R. Hult, and J. Fredriksson, "Quadratic approximation based heuristic for optimization-based coordination of automated vehicles in confined areas," in *2022 IEEE 61st Conference on Decision and Control (CDC)*. IEEE, 2022, pp. 6156–6162.

[15] S. A. Fayazi and A. Vahidi, "Mixed-integer linear programming for optimal scheduling of autonomous vehicle intersection crossing," *IEEE Transactions on Intelligent Vehicles*, vol. 3, no. 3, pp. 287–299, 2018.

[16] M. Kneissl, A. Molin, S. Kehr, H. Esen, and S. Hirche, "Combined scheduling and control design for the coordination of automated vehicles at intersections," *IFAC-PapersOnLine*, vol. 53, no. 2, pp. 15 259–15 266, 2020.

[17] N. Murgovski, L. M. Johannesson, and B. Egardt, "Optimal battery dimensioning and control of a cvt phev powertrain," *IEEE Transactions on Vehicular Technology*, vol. 63, no. 5, pp. 2151–2161, 2013.

[18] A. Richards and J. How, "Mixed-integer programming for control," in *Proceedings of the 2005, American Control Conference, 2005.* IEEE, 2005, pp. 2676–2683.

[19] J. Nocedal and S. J. Wright, *Numerical optimization*. Springer, 1999.

[20] J. A. Andersson, J. Gillis, G. Horn, J. B. Rawlings, and M. Diehl, "Casadi: a software framework for nonlinear optimization and optimal control," *Mathematical Programming Computation*, vol. 11, no. 1, pp. 1–36, 2019.

[21] A. Wächter and L. T. Biegler, "On the implementation of an interior-point filter line-search algorithm for large-scale nonlinear programming," *Mathematical programming*, vol. 106, no. 1, pp. 25–57, 2006.